SUPPORTING INFORMATION

Microplastic Pollution in Benthic Midstream Sediments of the Rhine River

Thomas Mani,[†] Sebastian Primpke,[§] Claudia Lorenz,[§] Gunnar Gerdts,*[§] and Patricia Burkhardt-Holm*[†]

[†]Department of Environmental Sciences, The Man-Society-Environment Program, University of Basel, Vesalgasse 1, 4051 Basel, Switzerland

[§]Department of Microbial Ecology, Biologische Anstalt Helgoland, Alfred-Wegener-Institut Helmholtz-Zentrum für Polar- und Meeresforschung, Kurpromenade, 27498 Helgoland, Germany

This document contains:

15 Pages

11 Figures

3 Tables

ORDER OF CONTENTS

SI1 $ZnCl_2$ density separation and microplastic recovery experiments

As the specifically modified protocol for $ZnCl_2$ density separation (see section 2.3 of the manuscript) based on [1] used in this study has never been published, a recovery experiment was conducted to assess the efficiency of the protocol. Four size classes of Nile red-dyed, fluorescent polymethyl methacrylate (PMMA, ρ = 1.18 g cm^{-3}) fragments (62–125 µm, n = 40; 125–250 µm, n = 40; 250–500 µm, n = 20 and 500–1000 µm, n = 20) were separately mixed with 60 g of Rhine riverbed sediment (<2 mm). All size class experiments were executed in triplicate. After applying the $ZnCl_2$ separation protocol according to section 2.3, the supernatant was filtered onto cellulose filter paper (pore size: 3 µm, diameter: 25 mm; Rotilabo-Rundfilter Typ 115A, Carl Roth, Karlsruhe, Germany) and the recovered PMMA particles were visually counted using a fluorescence microscope (Nikon eclipse E 400, Nikon, Tokyo, Japan). Mean microplastic recovery (± SD) rates were 100.0 ± 0.0%, 90.0 ± 5.0%, 80.8 ± 6.3%, and 55.0 ± 8.7% for the 500–1000 µm, 250–500 µm, 125–250 µm, and 62–125 µm size classes, respectively (Figure S5).

SI2 Blank correction of riverbed sediment microplastic concentrations

Three procedural blanks were run to detect any sample processing-induced microplastics in the samples. The $ZnCl_2$ density separation (section 2.3 of the manuscript), Fenton's reagent (2.4), focal plane array µFTIR (2.5) and automated analysis of µFTIR data (2.6) were performed without sediment samples. The resulting synthetic polymer abundances (average 97.3 ± 63.7 MP particles per blank) were subsequently subtracted from the microplastic concentrations determined for the Rhine riverbed samples in the respective polymer proportions (Table S1). The microplastic counts for the aliquots of pooled sample analyzed (n = 10) by micro-Fourier-transform infrared spectroscopy (µFTIR) were blank corrected by subtracting the average blank microplastic count (97.34, n = 3), before extrapolating to the microplastic count for the total volume (100%) of each sediment sample. Microplastic concentrations (MP kg^{-1} sediment)

were then calculated based on the dry sediment weight (*cf.* Electronic Supporting Information, ESI).

SI3 Error propagation calculated values derived via FTIR imaging

The following equation was used to calculate the errors for the single samples based on the number of particles (N_P), mass dw (m_S) and the aliquot fractions for the Anodisc-Filtration (f):

$$\Delta N_{DW} = \sqrt{\left(\frac{N_P}{-m_S^2 f}\,\Delta m_S\right)^2 + \left(\frac{N_P}{m_S - f^2}\,\Delta f\right)^2 + \left(\frac{1}{m_S f}\,\Delta N_P\right)^2} \quad (1)$$

The error of the determined value ΔN_{DW} is calculated under the following assumptions: (i) dw sediment Δm_S is weighed at an accuracy of +/- 1 g (section 2.2.); (ii) sub-aliquot volumes for Anodisc-filtration (Δf) was assessed at an accuracy of +/- 1% (2.4.); (iii) FTIR MP particle count accuracy (ΔN_P) is +/- 5% (2.6.).

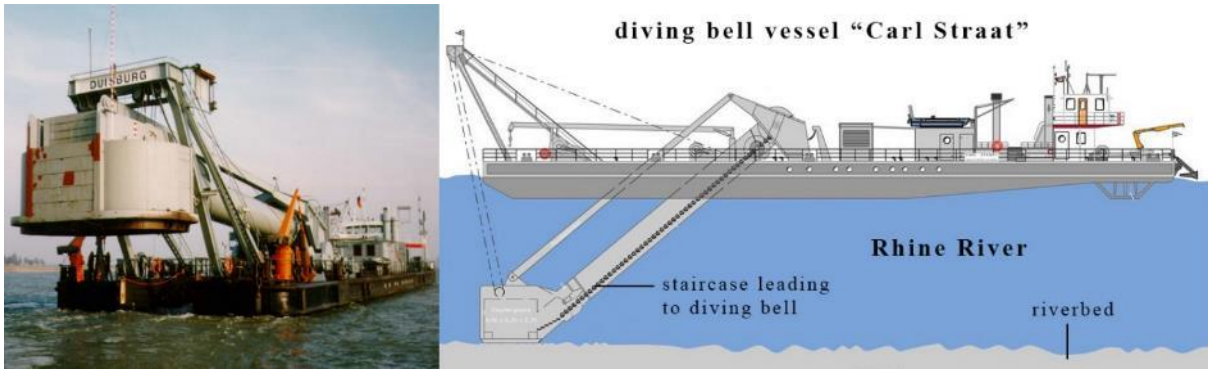

Figure S1: Diving bell vessel "Carl Straat". The riverbed can be accessed by foot through a staircase and diving bell that is open on the bottom. Water is kept out using a double door system and artificial adjustment of air pressure in the bell and staircase (0.1 bar per 1.02 m water depth). Images courtesy of the German Waterways and Shipping Administration (WSV), department Duisburg, modified.

Figure S2: Bucket chain (left arrow, A) vessel with accompanying transport barge (right arrow, A) with the Rhine River visible in the background at Rees, Germany (A). Bucket chain (centre) in action dredging riverbed sediments (direction of hauling: upwards, B). Close-up of sand-gravel riverbed sediment in the dredge bucket (C).

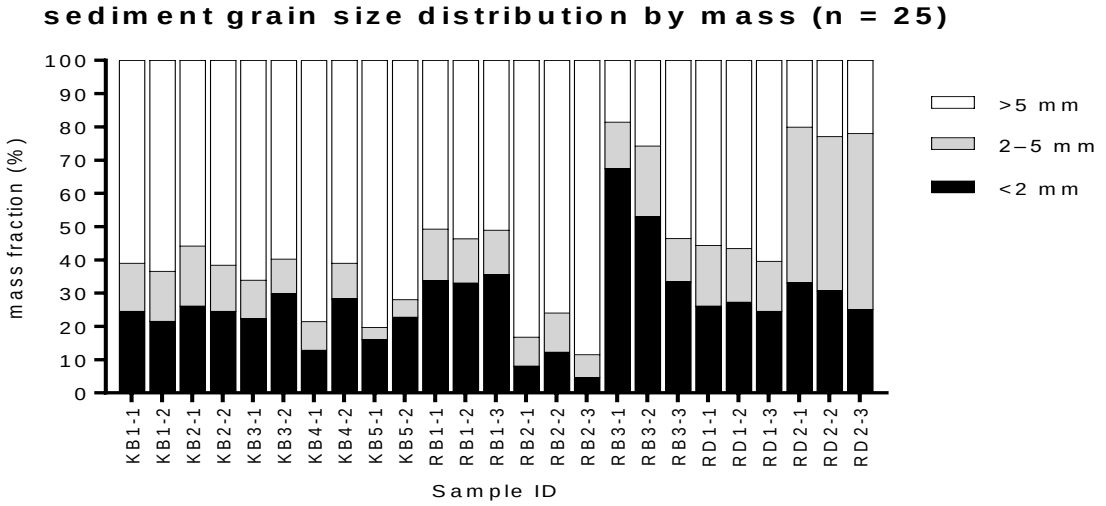

Figure S3: Percentage mass fractions of grain size classes (>5 mm, 2–5 mm and <2 mm) in the 25 Rhine riverbed sediment samples. K = Koblenz; R = Rees; B = diving bell; D = bucket chain dredger.

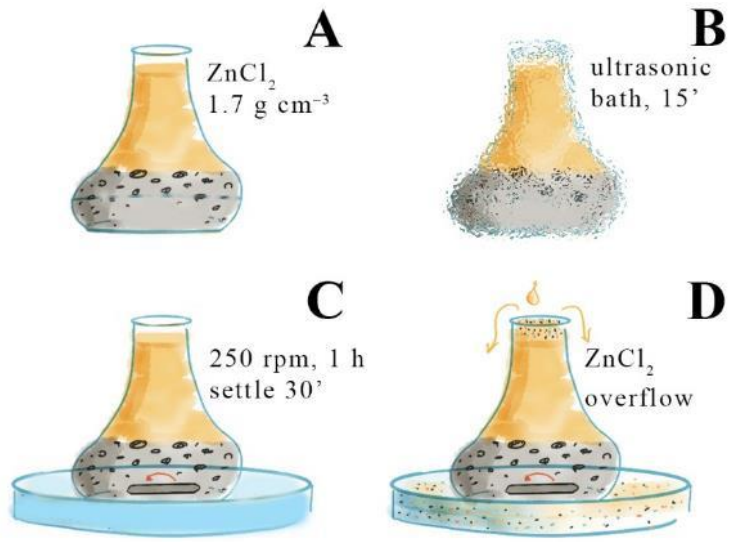

Figure S4: Schematic depiction of density separation using $ZnCl_2$ (ρ ~1.7 g cm^{-3}) (adapted from [1]). Dry sample was added to an Erlenmeyer flask (100 mL) and the receptacle was topped up with $ZnCl_2$, leaving a 1.5 cm margin below the brim (A). The sealed Erlenmeyer flask was submerged in an ultrasonic bath until the mouth of the flask was 3 cm above the water line and sonicated at 160 W/35 kHz for 15 min (B). Then, the sample was stirred for 1 h at 250 rpm using a PTFE-coated magnetic stirrer bar. The exterior of the flask was cleaned with distilled water (Aq. dest.), and the flask was placed onto a 14 cm-diameter Petri dish (C). The flask was completely topped up with $ZnCl_2$, the contents were allowed to settle for 30 min, then an additional 20 mL of $ZnCl_2$ was added, inducing overflow of excess liquid and the suspended solids therein into the underlying Petri dish (D).

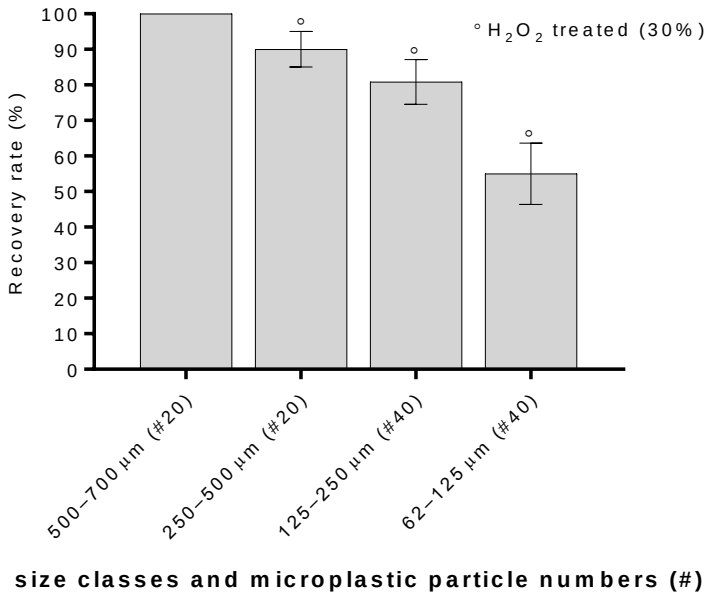

Figure S5: Density separation spike-recovery experiment (n = 3) using $ZnCl_2$ (ρ ~1.7 g cm^{-3}) and polymethylmethacrylate (PMMA, ρ 1.18 g cm^{-3}) microplastic particles (62–700 µm). Hashes (#) indicate the number of spiked PMMA particles. All size classes were investigated in triplicate. Error bars indicate standard deviation. Circles above the error bars indicate overnight H_2O_2 treatment (30%).

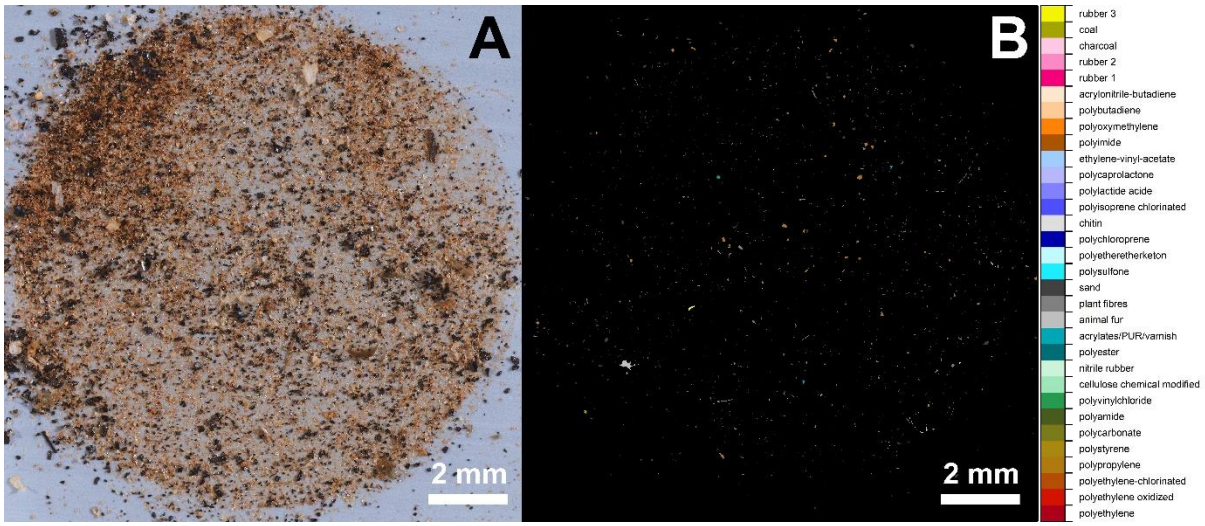

Figure S6: Visual overview (A) and false colour µFTIR image (B) of the sample filtrate for site RB3, Rees.

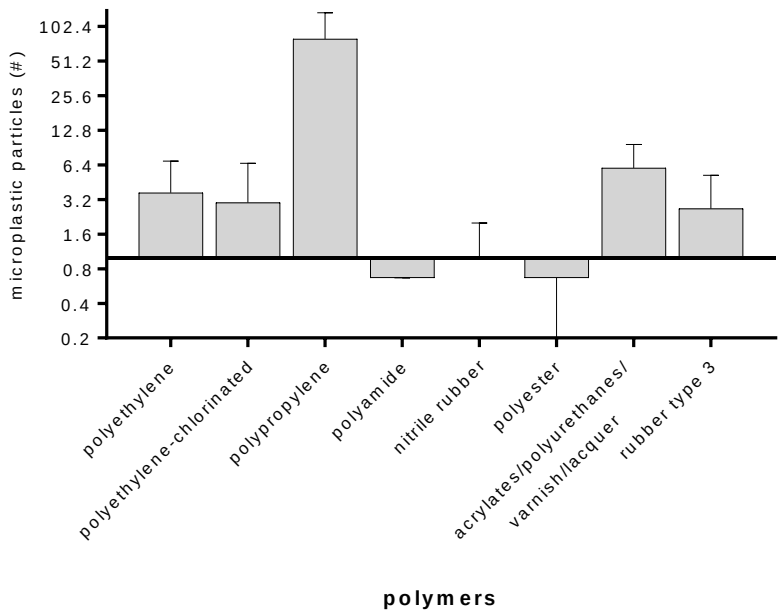

Figure S7: Mean microplastic particle abundance in the procedural blanks (n = 3). Error bars indicate standard deviation. The y-axis is log2 scaled; 0.67 particles of polyamide and polyester and one nitrile rubber particle were detected.

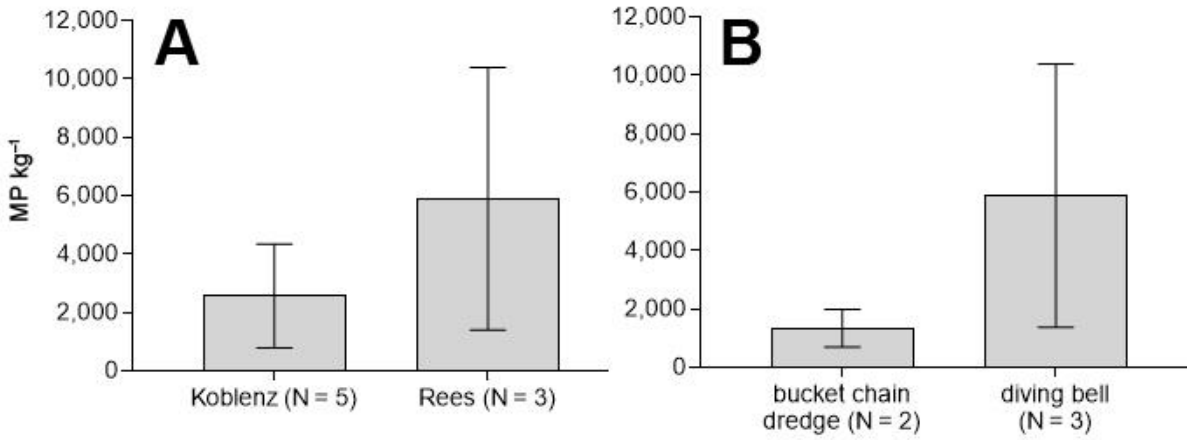

Figure S8: Mean microplastic concentrations in riverbed sediments (MP kg^{-1}) compared by location, Koblenz vs. Rees (A), and riverbed sampling access mode (B). The access mode was compared at Rees as this was the only location where both were applied (B). Error bars indicate standard deviation. No significant differences were identified (unpaired t-test with Welch's correction, $p > 0.05$).

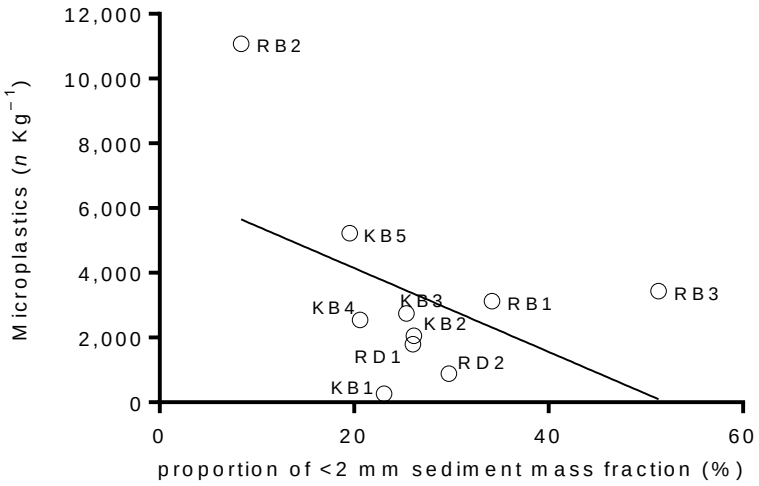

Figure S9: Linear regression of microplastic concentrations (MP kg^{-1}) and proportion of sand (< 2 mm, %) in the respective sample pool. R square = 0.22; $p = 0.17$. The proportion of sand in the sample was used as a proxy for near-riverbed deposition and flow dynamics.

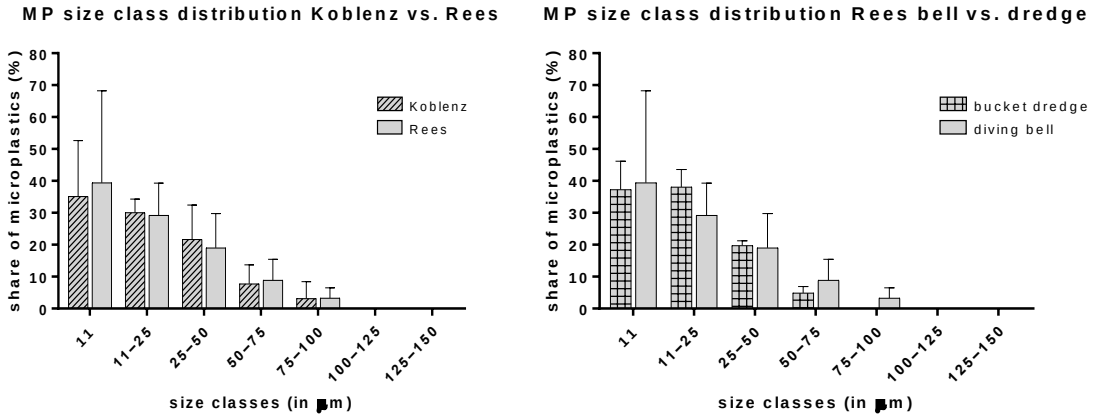

Figure S10: Size class distribution for the microplastics (< 500 µm) identified in all 10 sample pools ($n = 25$) compared by sampling location (Koblenz vs. Rees, left panel) and by sampling method (bucket chain dredger vs. diving bell, right panel). Size classes < 11–150 µm were considered.

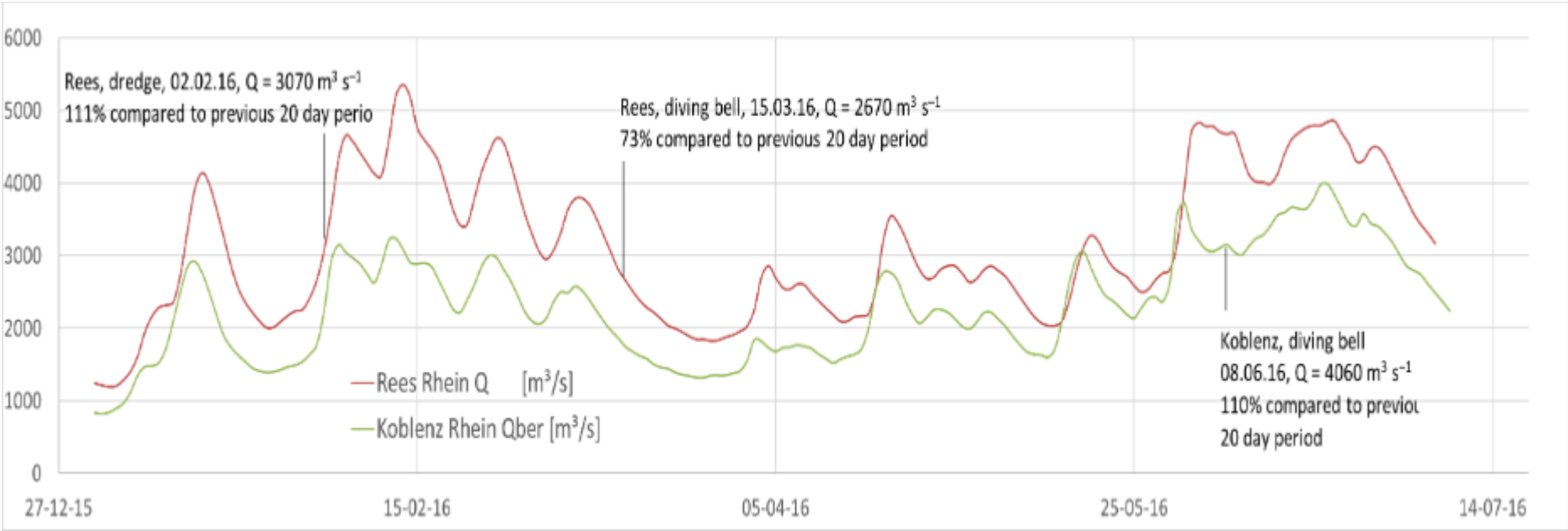

Figure S11: Rhine River discharge (Q in $m^3\ s^{-1}$) at Rees (Rh-km 837.4, red line) and at Bonn (Rh-km 654.8, 56.03 km downstream of the Koblenz sampling sites, blue line) between 01.01.2016 and 08.07.2016. Bucket chain dredge sampling at Rees on 02.02.2016 and diving bell sampling at Rees on 15.03.2016 and Koblenz on 08.06.2016 are indicated [2].

Table S1: Sediment sample metadata.

ID[A]	Coordinates	Rhine-kilometre (Rh-km)	Sampling date	Water depth (cm)	Sed. Depth (cm)	Sample ww (g)	Sample dw (g)	Fractions dw (mm, %)			Sample vol. (cm^3)[B]	On Anodic for µFTIR (%)[C]	MP conc. (× 10^3 MP kg^{-1})
								<2	2–5	>5			
KB1-1	N 50°22’47.25	593.95	08.06.2016	700	7	1637	1493	24.6	14.5	61.0	553	100.0	0.26 ± 0.01
KB1-2	E 7°36’50.74			700	7	1773	1596	21.6	15.0	63.4	591		
KB2-1	N 50°22’46.92	593.95	08.06.2016	650	7	1437	1387	26.2	18.1	55.7	501	58.3	2.74 ± 0.15
KB2-2	E 7°36’44.71			650	7	1358	1323	24.6	13.9	61.5	471		
KB3-1	N 50°23’10.82	594.8	08.06.2016	650	7	1372	1274	22.4	11.5	66.0	405	26.0	2.05 ± 0.13
KB3-2	E 7°36’29.68			650	7	1433	1312	29.9	10.4	59.7	452		
KB4-1	N 50°24’0.91	597.05	08.06.2016	650	7	1464	1336	12.9	8.6	78.5	441	91.2	2.54 ± 0.14
KB4-2	E 7°35’8.19			650	7	1625	1404	28.3	10.7	61.0	513		
KB5-1	N 50°24’42.43	598.77	08.06.2016	650	7	1617	1481	16.2	3.6	80.2	546	7.5	5.22 ± 0.75
KB5-2	E 7°34’10.37			650	7	1749	1556	22.9	5.2	71.9	589		
RB1-1	N 51°45’23.47	837.41	15.03.2016	750	7	950	878	33.7	15.6	50.7	325	7.6	3.13 ± 0.44
RB1-2	E 6°23’42.27			750	7	1145	1080	33.1	13.2	53.6	396		
RB1-3				750	7	1461	1162	35.6	13.3	51.0	437		
RB2-1	N 51°45’20.11	837.41	15.03.2016	750	7	851	812	8.1	8.7	83.1	304	67.9	11.07 ± 0.6
RB2-2	E 6°23’42.28			750	7	894	845	12.3	11.8	75.9	410		
RB2-3				750	7	1097	1058	4.7	6.8	88.5	385		
RB3-1	N 51°45’14.64	837.41	15.03.2016	500	7	952	817	67.6	14.0	18.5	330	77.9	3.43 ± 0.19
RB3-2	E 6°23’40.40			500	7	970	859	53.0	21.3	25.7	426		
RB3-3				500	7	1205	1140	33.4	13.1	53.5	446		
RD1-1	N 51°45’18.68	837.52	02.02.2016	577	42	1368	1297	26.2	18.2	55.6	497	42.1	1.79 ± 0.1
RD1-2	E 6°23’35.60			577	42	1424	1408	27.3	16.1	56.5	532		
RD1-3				577	42	1366	1326	24.6	15.1	60.3	522		
RD2-1	N 51°45’17.87	837.52	02.02.2016	508	111	1291	1226	33.3	46.7	20.0	450	53.2	0.89 ± 0.05
RD2-2	E 6°23’35.59			508	111	1245	1195	30.8	46.4	22.8	450		
RD2-3				508	111	1279	1238	25.2	52.9	21.9	511		

[A] K = Koblenz; R = Rees; B = diving bell; D = bucket chain dredger.

[B] Net sample volume determined by porosity assessment, described in section 2.2 of the main article.

[C] Percentage of $ZnCl_2$ density separation supernatant filtered onto the Anodisc (0.22 µm) and analyzed by FPA µFTIR.

Table S2: Literature overview of microplastics in benthic and littoral sediments of lotic waterbodies.

Lotic waterbody	Compart-ment	MP conc. ($\times 10^3$ MP kg^{-1})	MP size (µm)	Sampling method	MP identification	Reference
St. Lawrence River, including lakes (Canada, CA)	Benthos	0–1.5	400–2160	Petite Ponar Grab; Peterson Grab;10 sites	Visual selection, diff. scanning calorimetry (*n* = n.a.)	[3]
Wen-Rui Tang River estuary (China, CN)	Benthos	18.69–74.8	20–5000	Peterson grab; 12 sites	Visual selection, µFTIR (*n* = 595)	[4]
Yangtze River (CN)	Benthos	0.03–0.3	48–5000	Van Veen Grab; 29 sites	Visual selection, µRaman (*n* = 174)	[5]
Amsterdam canals (Netherlands, NL)	Benthos	0.07–10.5	10–5000	Van Veen Grab; 6 sites	Visual selection, µFTIR (subsample 6%)	[6]
Rhine estuary, Port of Rotterdam (NL)	Benthos	3.01–3.6	10–5000	Van Veen Grab; 2 sites	Visual selection, µFTIR (subsample 6%)	[6]
18 rivers or channels in Irwell and Upper Mersey catchments (UK)	Benthos	0.3–4.8	79–4779	Cylinder resuspension technique; 40 sites	Visual selection, FTIR (*n* = 100)	[7]
Leach, Lambourn and Cut rivers (UK)	Benthos	0.19 ± 0.04–0.66 ± 0.08	1000–4000	Stainless steel spoon; 4 sites	Raman (*n* = 336)	[8]
Bloukrans River System (South Africa, ZA)	Benthos	0.006 ± 0.004–0.16 ± 0.14	63–5000	Quadrat and hand device; 30 sites	Comprehensive visual selection and identification	[9]
Rhine (DE)	Benthos	0.26 ± 0.01–11.07 ± 0.6	11–5033	Quadrat and steel hand spade; 10 sites	FPA µFTIR; visual selection ATR-FTIR (> 500 µm)	Present study
L. Ontario trib., Don, Humber, Etobicoke, Red Hill (CA)	Littoral	0.04–27.83	63–2000	Petite Ponar Grab; 7 sites	Raman (*n* = 90)	[10]
Ottawa River (CA)	Littoral	0.11–0.45	>100	Ekman bottom grab sampler; 10 sites	Comprehensive visual selection and identification	[11]
Beijiang River (CN)	Littoral	0.18 ± 0.07–0.54 ± 0.11	1–5000	Quadrat and stainless steel shovel; 8 sites	Comprehensive visual selection and µFTIR	[12]
Seven rivers or channels in the Shanghai urban area (CN)	Littoral	0.05 ± 0.01–1.6 ± 0.19	>1	quadrat and shovel; 7 sites	µFTIR (*n* = n.a.)	[13]
Rhine, Main (DE)	Littoral	0.23–3.76	63–5000	Stainless steel spoon	ATR-FTIR (*n* = n.a.)	[14]
Elbe, Mosel, Neckar, Rhine (DE)	n.a.	0.03–0.06	n.a.	n.a.	n.a.	[15]

Table S3: Numerical proportions of polymer types by total MP concentrations (MP kg^{-1}), ordered by number of sites of occurrence from left to right.

Site	Total ($\times 10^3$ MP kg^{-1})	(%)																	
		APV*	CPE	EPDM*	PEST*	PE	PS*	PA*	NR	EVA	Rubber	PP	CMC*	OPE	PC*	PVC*	PCP	PLA*	ACNB*
KB1	0.26 ± 0.01	77.07	0.00	0.00	0.00	16.66	0.00	0.00	0.00	0.00	6.26	0.00	0.00	0.00	0.00	0.00	0.00	0.00	0.00
KB2	2.74 ± 0.15	75.70	1.07	5.87	5.84	2.14	0.00	0.64	0.00	0.00	0.00	4.57	1.04	0.00	0.00	0.00	0.00	3.12	0.00
KB3	2.05 ± 0.13	64.31	2.05	0.00	24.52	0.00	0.00	0.00	2.86	0.00	6.26	0.00	0.00	0.00	0.00	0.00	0.00	0.00	0.00
KB4	2.54 ± 0.14	85.18	2.50	3.50	2.66	0.85	0.00	0.72	0.28	2.87	0.72	0.00	0.00	0.00	0.00	0.72	0.00	0.00	0.00
KB5	5.22 ± 0.75	83.12	0.00	0.00	4.14	0.00	12.74	0.00	0.00	0.00	0.00	0.00	0.00	0.00	0.00	0.00	0.00	0.00	0.00
RB1	3.13 ± 0.44	38.90	0.00	13.26	0.00	12.91	27.95	0.00	0.00	6.99	0.00	0.00	0.00	0.00	0.00	0.00	0.00	0.00	0.00
RB2	11.07 ± 0.6	81.77	0.66	0.98	0.00	0.00	0.00	1.01	0.96	1.11	0.00	0.00	12.19	0.44	0.66	0.00	0.22	0.00	0.00
RB3	3.43 ± 0.19	33.40	0.60	1.22	0.62	0.60	1.25	1.55	0.46	1.87	1.25	57.18	0.00	0.00	0.00	0.00	0.00	0.00	0.00
RD1	1.79 ± 0.1	78.47	6.03	8.85	4.10	0.35	2.20	0.00	0.00	0.00	0.00	0.00	0.00	0.00	0.00	0.00	0.00	0.00	0.00
RD2	0.89 ± 0.05	78.29	3.93	9.74	0.00	0.00	0.00	0.00	0.00	0.00	0.00	4.50	0.00	0.00	0.00	0.00	0.00	0.00	3.53

APV: acrylates/polyurethanes/varnish cluster; CPE: chlorinated polyethylene; EPDM: ethylene-propylene-diene rubber; PEST: polyester; PE: polyethylene; PS: polystyrene; PA: polyamide; NR: nitrile rubber; EVA: ethylene-vinyl-acetate; PP: polypropylene; CMC: chemically modified cellulose; OPE: oxidised polyethylene; PC: polycarbonate; PVC: polyvinylchloride; PCP: polychloroprene; PLA: polylactide acide; ACNB: acrylonitrile-butadiene.
* specific density >1 g cm^{-1}

REFERENCES

(1) Imhof, H. K.; Schmid, J.; Niessner, R.; Ivleva, N. P.; Laforsch, C. A novel, highly efficient method for the separation and quantification of plastic particles in sediments of aquatic environments. *Limnol. Oceanogr. Meth.* **2012**, *10*, 524–537; DOI: 10.4319/lom.2012.10.524.

(2) WSV DE. *Abflussdaten Tagesmittel Rees und Bonn*, 2016. http://undine.bafg.de/.

(3) Castañeda, R. A.; Avlijas, S.; Simard, M. A.; Ricciardi, A.; Smith, R. Microplastic pollution in St. Lawrence River sediments. *Can. J. Fish. Aquat. Sci.* **2014**, *71*, 1767–1771; DOI: 10.1139/cjfas-2014-0281.

(4) Wang, Z.; Su, B.; Xu, X.; Di Di; Huang, H.; Mei, K.; Dahlgren, R. A.; Zhang, M.; Shang, X. Preferential accumulation of small (<300 μm) microplastics in the sediments of a coastal plain river network in eastern China. *Water res.* **2018**, *144*, 393–401; DOI: 10.1016/j.watres.2018.07.050.

(5) Di, M.; Wang, J. Microplastics in surface waters and sediments of the Three Gorges Reservoir, China. *Sci. Tot. Env.* **2018**, *616-617*, 1620–1627; DOI: 10.1016/j.scitotenv.2017.10.150.

(6) Leslie, H. A.; Brandsma, S. H.; van Velzen, M. J. M.; Vethaak, A. D. Microplastics en route: Field measurements in the Dutch river delta and Amsterdam canals, wastewater treatment plants, North Sea sediments and biota. *Environ. Int.* **2017**, *101*, 133–142; DOI: 10.1016/j.envint.2017.01.018.

(7) Hurley, R.; Woodward, J.; Rothwell, J. J. Microplastic contamination of river beds significantly reduced by catchment-wide flooding. *Nat. Geosci.* **2018**, *11*, 251–257; DOI: 10.1038/s41561-018-0080-1.

(8) Horton, A. A.; Svendsen, C.; Williams, R. J.; Spurgeon, D. J.; Lahive, E. Large microplastic particles in sediments of tributaries of the River Thames, UK - Abundance, sources and methods for effective quantification. *Marine pollution bulletin* **2017**, *114*, 218–226; DOI: 10.1016/j.marpolbul.2016.09.004.

(9) Nel, H. A.; Dalu, T.; Wasserman, R. J. Sinks and sources: Assessing microplastic abundance in river sediment and deposit feeders in an Austral temperate urban river system. *Sci. Tot. Env.* **2018**, *612*, 950–956; DOI: 10.1016/j.scitotenv.2017.08.298.

(10) Ballent, A.; Corcoran, P. L.; Madden, O.; Helm, P. A.; Longstaffe, F. J. Sources and sinks of microplastics in Canadian Lake Ontario nearshore, tributary and beach sediments. *Marine pollution bulletin* **2016**, *110*, 383–395; DOI: 10.1016/j.marpolbul.2016.06.037.

(11) Vermaire, J. C.; Pomeroy, C.; Herczegh, S. M.; Haggart, O.; Murphy, M.; Schindler, D. E. Microplastic abundance and distribution in the open water and sediment of the Ottawa River, Canada, and its tributaries. *FACETS* **2017**, *2*, 301–314; DOI: 10.1139/facets-2016-0070.

(12) Wang, J.; Peng, J.; Tan, Z.; Gao, Y.; Zhan, Z.; Chen, Q.; Cai, L. Microplastics in the surface sediments from the Beijiang River littoral zone: Composition, abundance, surface textures and interaction with heavy metals. *Chemosphere* **2017**, *171*, 248–258; DOI: 10.1016/j.chemosphere.2016.12.074.

(13) Peng, G.; Xu, P.; Zhu, B.; Bai, M.; Li, D. Microplastics in freshwater river sediments in Shanghai, China: A case study of risk assessment in mega-cities. *Environmental pollution (Barking, Essex : 1987)* **2018**, *234*, 448–456; DOI: 10.1016/j.envpol.2017.11.034.

(14) Klein, S.; Worch, E.; Knepper, T. P. Occurrence and Spatial Distribution of Microplastics in River Shore Sediments of the Rhine-Main Area in Germany. *Environ. Sci. Technol.* **2015**, *49*, 6070–6076; DOI: 10.1021/acs.est.5b00492.

(15) Wagner, M.; Scherer, C.; Alvarez-Muñoz, D.; Brennholt, N.; Bourrain, X.; Buchinger, S.; Fries, E.; Grosbois, C.; Klasmeier, J.; Marti, T. *et al.* Microplastics in freshwater ecosystems: What we know and what we need to know. *Environ. Sci. Eur.* **2014**, *26*, 12; DOI: 10.1186/s12302-014-0012-7.